

Novel Boundary Condition for the Finite-Element Solution of Arbitrary Planar Junctions

M. I. Davanço, *Student Member, IEEE*, C. E. Rubio-Mercedes, and H. E. Hernández-Figueroa, *Senior Member, IEEE*

Abstract—A novel boundary condition for a two-dimensional finite-element method (2D-FEM) is developed to simulate accessing waveguides to planar optical junctions. This new boundary condition is based on a paraxial approximation to the field's derivatives over the junction's ports. The formulation is very easily adapted within the 2D-FEM framework while providing good simulation results. Two examples are provided to show the applicability and reliability of the present method: a waveguide step discontinuity and a sharp waveguide bend.

Index Terms—Finite-elements, mode-matching technique, perfectly matched layer, planar junctions, planar waveguides, waveguide discontinuities.

I. INTRODUCTION

IN THE simulation of optical junctions and discontinuities [1]–[3], a widely used technique for representing infinite accessing waveguides at the ports of a given structure consists of expanding the field over such ports in terms of the corresponding waveguides' modes [1]–[3]. An accurate boundary condition relating the field and its normal derivative then arises, which we call the Mode-Expansion Boundary Condition (MEBC) [1], [2]. Very recently, a new formulation was developed that combines a two-dimensional finite-element method (2D-FEM) and a beam-propagation method (BPM) through the MEBC with very interesting outcomes for structures bearing bidirectional propagation [3].

The technique involving the MEBC, however general and versatile, relies heavily on the calculation of many modes of the accessing waveguide, a procedure that both adds more complexity to the numerical framework and increases the processing time. In this letter, we propose a simpler boundary condition for the 2D-FEM, which permits to simulate accessing waveguides without the need of calculating waveguide modes, by using a paraxial approximation to the fields' longitudinal variation at the ports. This method, though not as general as the forementioned one, requires less computational effort and yields good results in a great number of cases. The new procedure itself is very simple and its integration within the 2D-FEM framework is quite straightforward. Also, it leads to more reliable outcomes—while maintaining the same sparsity—as the “simple” (impedance) boundary condition (SIBC)

Manuscript received June 23, 2000; revised October 11, 2000. This work was supported in part by the Brazilian agencies CAPES and CNPq.

The authors are with the University of Campinas, School of Electrical and Computer Engineering, Department of Microwaves and Optics, 13083-970, Campinas-SP, Brazil (e-mail: davanco@dmo.fee.unicamp.br; cosme@dmo.fee.unicamp.br; hugo@dmo.fee.unicamp.br).

Publisher Item Identifier S 1041-1135(01)00490-6.

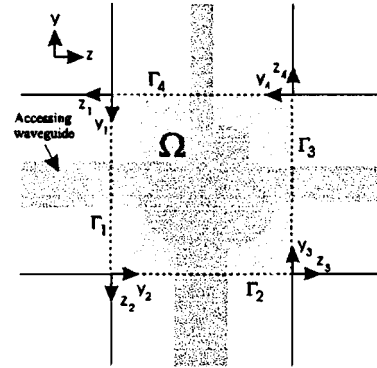


Fig. 1. Framework for finite-element analysis. The junction is inside region Ω , comprising four accessing waveguides.

in which only one mode is assumed to propagate along the access waveguides [4].

II. MODEL

We consider a planar (2-D) optical junction located inside the domain Ω in the yz -plane, as shown in Fig. 1, fed by (up to) four accessing waveguides. We use the same framework as in [3]. The boundary of the domain Ω is given by $\delta\Omega = \Gamma_1 + \Gamma_2 + \Gamma_3 + \Gamma_4$. To reduce the computational window, we used an extended frequency-domain version of perfectly matched layers (PMLs), with artificial electric and magnetic conductivities of parabolic profile, [5].

The scalar wave equation that models light propagation in Ω is taken directly from [1]. Application of Galerkin's method (with w as weight function) to such an equation leads to the weighted residual expression

$$\int_{\Omega} \left\{ \frac{p}{s_y^2} \frac{\partial w}{\partial y} \frac{\partial \phi}{\partial y} + \frac{p}{s_z^2} \frac{\partial w}{\partial z} \frac{\partial \phi}{\partial z} - q k_0^2 w \phi \right\} d\Omega = \sum_{l=1}^4 \int_{\Gamma_l} w \frac{\partial \phi}{\partial z_l} d\Gamma_l \quad (1)$$

where k_0 is the free space wavenumber and ϕ , p , q , s_z and s_y are the same as defined in [1].

In order to calculate the boundary integrals of (1), we express the field at the ports in terms of slowly varying envelopes, such that

$$\frac{\partial \phi(y_l, z_l)}{\partial z_l} = \left(\frac{\partial \phi}{\partial z_l} - j k_0 n_{0l} \phi \right) \exp(-j k_0 n_{0l} z_l) \quad (2)$$

where n_{0l} is the reference refractive index for port l .

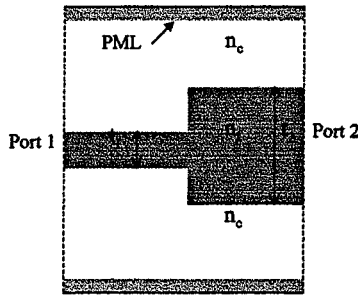


Fig. 2. Layout for step discontinuity simulation.

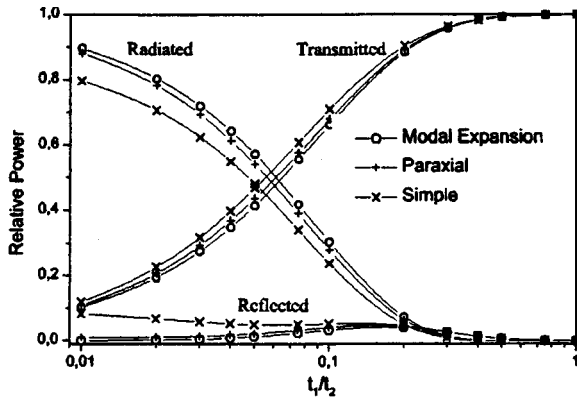


Fig. 3. Scattering characteristics for the step discontinuity.

Using this slowly varying approximation in the original 2-D wave equation, we obtain the following expression for the z -derivative of the envelope φ :

$$\frac{p}{s_z^2} \frac{\partial^2 \varphi}{\partial z_l^2} - 2jk_0 n_{0l} \frac{p}{s_z} \frac{\partial \varphi}{\partial z_l} + \frac{p}{s_y} \frac{\partial}{\partial y_l} \cdot \left(\frac{p}{s_y} \frac{\partial \varphi}{\partial y_l} \right) + k_0^2 (q - n_{0l}^2 p) \varphi = 0 \quad (3)$$

where the variation of p with respect to z_l is assumed to be zero. We next neglect the second z -derivative of φ in this expression, obtaining a Fresnel (paraxial) approximation to $\partial\varphi/\partial z_l$, which is replaced in (2). The resulting expression

$$\frac{p}{s_z} \frac{\partial \phi}{\partial z_l} = \frac{1}{2jk_0 n_{0l}} \left(\frac{p}{s_y} \frac{\partial}{\partial y_l} \left(\frac{p}{s_y} \frac{\partial \phi}{\partial y_l} \right) + k_0^2 (q + n_{0l}^2 p) \phi \right) \quad (4)$$

is then substituted into the boundary integrals in (1) and the rest of the discretization process follows in the usual way [4].

III. NUMERICAL EXAMPLES

A. Step Discontinuity

To show the applicability and reliability of the present method, we consider a step discontinuity as shown in Fig. 2, where $\lambda = 0.6328 \mu\text{m}$, $t_2 = \lambda/\pi$, $n_c = 1.0$, $n_f = \sqrt{5}$, and an incident fundamental TE mode is assumed on port 1 [1]. Fig. 3 shows the scattering parameters for the step as a function of the ratio t_1/t_2 . Comparing the results obtained with Paraxial Boundary Condition (PBC) and MEBC, it is confirmed that

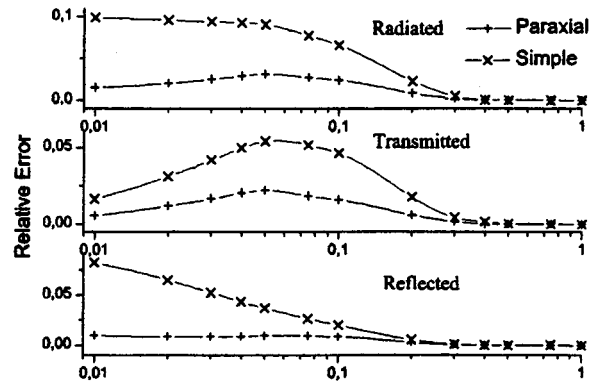
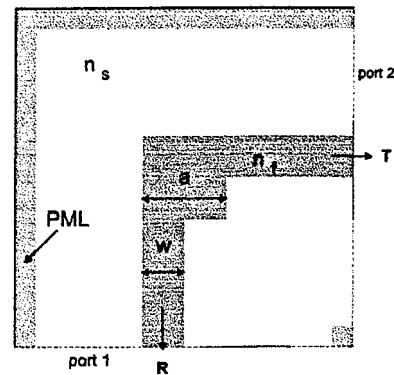


Fig. 4. Relative error for the step discontinuity.


 Fig. 5. Schematic of a 90° sharp waveguide bend with index $n = 3.2$ surrounded by air. $w = 0.2 \mu\text{m}$, $a = 0.62 \mu\text{m}$.

the new boundary condition allows for a reasonably good agreement. In Fig. 4, we display, respectively, the relative error of the calculated relative radiated, transmitted and reflected powers as a function of the ratio t_1/t_2 for the PBC and SIBC.

The error is calculated with respect to the more accurate MEBC results and shows that the PBC yields more accurate results than the SIBC. The error involved in the PBC method is due mostly to the presence of evanescent radiation modes at the ports, which are not accurately treated by the paraxial operator with real reference index [6] and, also, to the high index contrast, which leads to a wide spectrum. In this example, we have used 5000 quadratic triangular elements with 100 modes for the MEBC method and the effective index of the fundamental modes of the input-output (I/O) guides as reference indexes for the PBC and SIBC. The execution time for both PBC and SIBC methods is about ten times shorter than for the MEBC.

B. Sharp Bend

In this example, we consider a rectangular sharp bend with a square resonant cavity at the corner, as shown in Fig. 5 [7]. The waveguides used in this simulation have refractive index $n_f = 3.2$, width $w = 0.2 \mu\text{m}$, and are surrounded by air; such parameters are chosen to ensure single-mode operation over the entire excitation bandwidth. The side of the resonator defined in the schematic is $a = 0.62 \mu\text{m}$. In our simulation, MEBC with 100 modes is applied to the 2-D domain, discretized in 13 636 quadratic triangular elements.

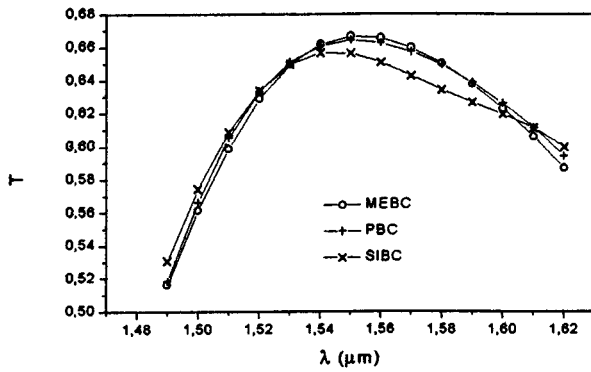


Fig. 6. Comparison of transmission of the waveguide bend calculated by using the MEBC, PBC, and SIBC in the 2D-FEM.

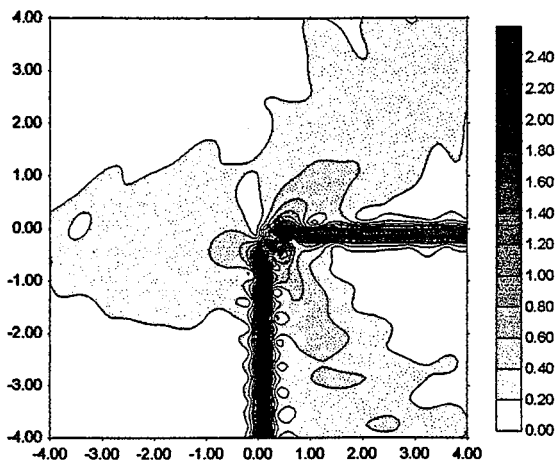


Fig. 7. Electric field amplitude in the waveguide bend with a resonator for $\lambda = 1.575 \mu\text{m}$, using PBC.

The relative transmitted power curve for this bend as a function of the wavelength is shown in Fig. 6 for an incident TE_0 mode on port 1, calculated with the three boundary conditions; results obtained with the MEBC agree quite well with those of [7], from which this example was taken. In this figure, it is apparent that results from the newly proposed method are in good agreement with those of the MEBC for all wavelengths tested, while those of the SIBC differ significantly for λ between $1.54 \mu\text{m}$ and $1.60 \mu\text{m}$. Fig. 7 shows the electric field amplitude for $\lambda = 1.575 \mu\text{m}$ obtained with the PBC, which compares well with the result computed with the MEBC. The result calculated with the SIBC, shown in Fig. 8, differs significantly from the previous one, specially in the radiative part of the field. This shows that the PBC constitutes a better alternative for representing accessing waveguides than the SIBC and should be more accurate in a larger set of cases.

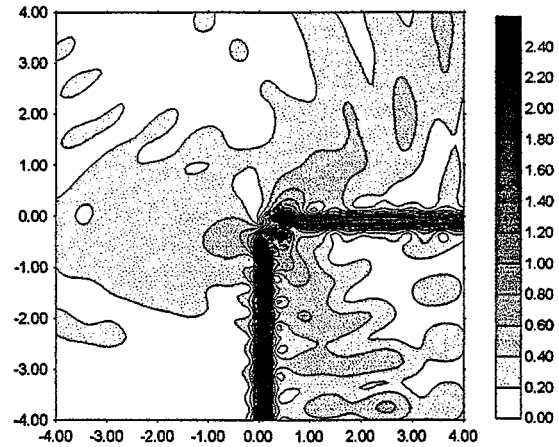


Fig. 8. Electric field amplitude in the waveguide bend with a resonator for $\lambda = 1.575 \mu\text{m}$, using SIBC.

IV. CONCLUSION

The implementation of the PBC is as simple as that of the SIBC and, therefore, much simpler than that of the MEBC. On the other hand, the final matrix system obtained with the PBC is as sparse as that obtained with the SIBC, therefore much less dense than that of the MEBC. As a reference, for the same problem, the computation time for the MEBC is, on average, ten times that for the others. We conclude that the PBC is a powerful boundary condition that may replace the MEBC in a great number of problems related to the simulation of planar optical junctions, with smaller computation times and a less complex implementation. Finally, even though the present technique has been used in 2-D examples, its extension to the 3-D cases is straightforward. In this situation, the computational gain will be much greater, since the spectral calculation for 2-D cross sections (for 3-D propagation) requires a much larger amount of effort than for the 1-D case (for 2-D propagation).

REFERENCES

- [1] M. Koshiba, *Optical Waveguide Theory by the Finite Element Method*. Tokyo, Japan: KTK Scientific, 1992.
- [2] M. Koshiba and K. Hirayama, "Application of the finite-element method to arbitrarily shaped discontinuities in a dielectric slab waveguide," *Proc. Inst. Elect. Eng.*, pt. H, vol. 135, no. 1, pp. 8–12, 1988.
- [3] S. Yoneta, M. Koshiba, and Y. Tsuji, "Combination of beam propagation method and finite element method for optical beam propagation analysis," *J. Lightwave Technol.*, vol. 17, pp. 2398–2404, Nov. 1999.
- [4] J. Jin, *The Finite Element Method in Electromagnetics*. New York: Wiley, 1993.
- [5] Ü. Pekel and R. Mittra, "A finite-element-method frequency-domain application of the perfectly matched layer (PML) concept," *Microwave Opt. Technol. Lett.*, vol. 9, no. 3, pp. 117–122, 1995.
- [6] H. E. Hernández-Figueroa, "Simple nonparaxial beam propagation method for integrated optics," *J. Lightwave Technol.*, vol. 12, pp. 644–649, Apr. 1994.
- [7] C. Manolatu, S. G. Johnson, S. Fan, P. R. Villeneuve, H. A. Haus, and J. D. Joannopoulos, "High-density integrated optics," *J. Lightwave Technol.*, vol. 17, pp. 1682–1692, Sept. 1999.